Received: 28 May 2025 | Accepted: 1 July 2025

DOI: 10.1002/ajb2.70093

SPECIAL ISSUE ARTICLE

Botany

Color polymorphism in *Anemone coronaria*: Correlations with soil, climate, and flowering phenology

Tzlil Labin[1] | **Banisha Phukela**[2] | **Tamar Keasar**[3] | **Nirit Lavie-Alon**[4] | **Yuval Sapir**[2]

[1]Department of Evolutionary & Environmental Biology, University of Haifa, Israel

[2]School of Plant Sciences & Food Security, Tel Aviv University, Israel

[3]Department of Biology & Environment, University of Haifa – Oranim, Israel

[4]Society for the Protection of Nature in Israel

Correspondence

Tzlil Labin, Department of Evolutionary & Environmental Biology, University of Haifa, Israel.
Email: labintzlil@gmail.com

This article is part of the *American Journal of Botany* special issue: "Paradigm Shifts in Flower Color."

Abstract

Premise: Flower color polymorphism (FCP) is thought to be driven by multiple selection agents. Although widely associated with visual attraction of multiple pollinators, FCP is also often correlated with abiotic factors. We explored the links between abiotic conditions, flowering phenology, and FCP in the winter-flowering geophyte *Anemone coronaria* L., which forms color-polymorphic or red-only populations.

Methods: We mapped the geographical distribution of color diversity in *A. coronaria* in Israel using citizen-science data. We recorded the phenology and density of red and non-red flowers during two flowering seasons in 18 plots along a rainfall gradient. We related the spatiotemporal data to soil and climate measures.

Results: Color-polymorphic populations are restricted to Mediterranean sites (>450 mm annual rainfall, >60% soil saturation), whereas red populations are found in Mediterranean and in semiarid sites, and in soils with high (>15%) soil calcium carbonate ($CaCO_3$) content. Greater soil electrical conductance (salts and water) was predictive of earlier first flowers. Flowering started earlier in Mediterranean than in semiarid plots, and earlier in non-red than in red flowers. Temperature and soil potassium concentrations (for non-red flowers) or sand content (for red flowers) were predictive of the timing of peak flowering.

Conclusions: The spatiotemporal patterns of FCP in *A. coronaria* may reflect adaptation of red flowers to stressful semiarid abiotic conditions and to pollinator preferences. Abiotic conditions that delay flowering may benefit red anemones by enhancing their probability of encountering glaphyrid beetles, their specialized pollinators.

KEYWORDS

abiotic, $CaCO_3$, citizen science, edaphic factors, flower color polymorphism, Mediterranean, phenology, rainfall, Ranunculaceae, temperature

Flower color is an important trait in plants, often associated with pollinator attraction and reproduction. While many plant species are monomorphic in flower color, flowers of several other species vary in color (Sapir et al., 2021). Flower color polymorphism (FCP) is a discrete or gradual variation in flower color, often genetically inherited, within or between natural populations of a species (Narbona et al., 2017). Much research attention has focused on biotic selection agents that contribute to flower color variation (Sapir et al., 2021). These polymorphisms are commonly attributed to balancing pollinator-mediated selection, which is driven by preferences of multiple pollinators to specific colors and their contribution to plant reproductive success (Dafni et al., 2020; Trunschke et al., 2021; Wang et al., 2024). Similarly, herbivore preferences for specific color morphs, with pollinator preferences, can support FCP

(Strauss and Whittall, 2016; Vaidya et al., 2018; Saabna et al., 2025).

Abiotic factors can also be selection agents, in addition to pollinator-mediated selection and pleiotropic effects of the pigments, which maintain color variation (Sapir et al., 2021). Particular floral colors within and among species have been linked to enhanced tolerance to abiotic stressors (Winkel-Shirley, 2002; Arista et al., 2013; Strauss and Whittall, 2016; Peach et al., 2020) and to environmental conditions, such as temperature, UV radiation, rainfall, soil moisture, and soil fertility that vary over time and space (Horovitz, 1985; Koes et al., 1994; Schemske and Bierzychudek, 2007; Sullivan and Koski, 2021; Dai et al., 2022; Mtileni et al., 2024; Rodríguez-Castañeda et al., 2024). Anthocyanin pigments may have evolved in plant tissues in response to high UV radiation, drought stress, and herbivory, later appearing in flowers (Rudall, 2019). These floral pigments often provide stress adaptations, while also attracting pollinators (Gonzalez, 2009; Dick et al., 2011; Arista et al., 2013). For example, flowers with higher pigment concentration have been found to be better adapted to frost, heat and drought (Dick et al., 2011; Ortiz et al., 2015; Berardi et al., 2016). Complementarily, lower tolerance to heat and drought was found in white and unpigmented flowers, which perform better in mesic sites (Coberly and Rausher, 2003; Tang and Huang, 2010; Tang et al., 2016). Such differential climate adaptations may generate a geographic segregation of flower color morphs (Schemske and Bierzychudek, 2007; Dick et al., 2011; Arista et al., 2013). Overall, the interplay between biotic (pollinators, herbivores) and abiotic (soil, climate) selection agents, and even neutral processes, drive and maintain FCP (Strauss and Whittall, 2016; Narbona et al., 2017; Sapir et al., 2021).

Flower color polymorphism can manifest itself as several color morphs within the same area, different color morphs in adjacent areas, or as different morphs that occupy separate areas. Consequently, polymorphism may exist in some populations, while monomorphism dominates others (Narbona et al., 2017; Dafni et al., 2020). Moreover, color frequencies often vary between polymorphic populations (Bolton et al., 2015; Imbert, 2021). Interestingly, all known cases of FCP in the Mediterranean basin consist of both poly- and monomorphic populations (Narbona et al., 2017). What environmental factors are predictive of the color display (mono- or polymorphic) of any specific population of Mediterranean species with FCP? Here, we address this question for *Anemone coronaria* L. (Ranunculaceae), a widespread Mediterranean color-polymorphic geophyte.

Color-associated differences in flowering phenology may contribute to FCP through assortative mating, potentially promoting partial reproductive isolation between color morphs. For instance, the yellow morph of *Opuntia streptacantha* reaches peak bloom earlier than the orange one (Manzanarez-Villasana and Mandujano, 2024), and the white morph of *Ophiorrhiza japonica* flowers earlier than the pink morph (Wang et al., 2024). Similarly, flowering onset of the blue morph of *Lysimachia arvensis* is earlier than that of the red morph. This phenological difference is unaffected by environmental conditions, suggesting that the timing of flowering in both color morphs is genetically controlled (Arista et al., 2013). The abiotic factors that influence the timing of flowering in species with FCP are not sufficiently understood. Therefore, we also explored how abiotic factors affect color-associated phenology in *A. coronaria*.

Anemone coronaria is a widespread Mediterranean geophyte with a broad array of genetically inherited floral colors and numerous color variations across its distribution, making it ideal to study FCP in the context of environmental interactions. The main floral color morphs are white, blue/purple, and red (scarlet), produced by at least four epistatic genes: *Alb* (albino), *Sc* (scarlet), *W* (white), and *B* (blue) (Dafni et al., 2020). The albino display is created by the *Alb/Alb* genotype, which blocks the production of anthocyanins in all parts of the plant including the otherwise dark anthers. This gene is epistatic over all others. The red color is produced by a pair of recessive alleles *sc/sc*, while non-red plants carry the dominant *Sc* allele. Non-red homozygous *Sc/Sc* genotypes produce flowers of uniform color, whereas the heterozygous genotype *Sc/sc* can produce either uniformly non-red colored flowers, or flowers with sparse red spots. Purple and blue are dominant over white (Horovitz, 1975, 1995; Yonash et al., 2004; Keasar et al., 2010). The flowering season starts as early as late November, several weeks after the first rains of the wet season. It lasts until April, a month with declining rainfall, increasing temperatures, and drying soil, just before the dry season begins. An individual flower lasts for 10–14 days, although high day temperatures accelerate flower development. In Israel, color-polymorphic populations are limited to the center and north of the country, which has a Mediterranean climate. Red populations grow across the country, including the arid and semiarid regions in its south.

Pollinators also play a role in maintaining FCP in *A. coronaria* through their foraging preferences (Keasar et al., 2010; Dafni et al., 2020; T. Labin et al., unpublished data). In a controlled field experiment, most pollinators visited white and purple flowers early in the flowering season in a northern site, while red flowers were mostly visited late in the season in the south (T. Labin et al., unpublished data). Nevertheless, environmental factors were also proposed to underlie the floral color of *A. coronaria* (Horovitz, 1975, 1976). The red morph was hypothesized to be better adapted to xeric conditions and to chalk and marl soils, which could be associated with low water-holding capacity (Horovitz, 1975; Dafni et al., 2020). Horovitz (1975) further suggested that non-red morphs perform poorly on chalk substrates and that low rainfall and high temperatures also limit their distribution. These hypotheses were never tested.

While the different color morphs can flower simultaneously, their proportions within the polymorphic populations fluctuate over the season (Horovitz, 1975; Keasar et al., 2010). Polymorphic populations start and end their bloom earlier than red populations. Due to these differences, non-red flowers dominate early in the season, while only red flowers bloom late in the season (Horovitz, 1985).

These past descriptions of the plant's flowering ecology did not include any quantitative account of flowering phenology across sites and color morphs or in relation to environmental factors.

The geographic and temporal flowering patterns of *A. coronaria*'s color morphs seem to reflect a complex interplay between genetic, abiotic, and biotic factors. While the contribution of biotic agents such as herbivores or pollinators in maintaining FCP in *A. coronaria* has been previously studied, the putative role of abiotic factors has not been quantified (Horovitz, 1991; Keasar et al., 2010; Dafni et al., 2020; Keasar and Labin, 2025; Saabna et al., 2025). In this study, we first described in detail the complex spatial and temporal flowering pattern of the color morphs of *A. coronaria*. We then tried to unravel the relationship between abiotic characteristics (rainfall average and accumulation; minimum, maximum, and mean temperatures; various soil variables) and flowering phenology.

MATERIALS AND METHODS

Surveys by citizen scientists

An online survey form for data collection was established in 2019, in collaboration with The Society for the Protection of Nature in Israel (SPNI). The platform (Appendix S1: Figure S1) allowed the public to upload reports of flowering *A. coronaria* across Israel. The form instructed the participants to select a 10 × 10 m square plot, or, alternatively, to walk a 50 × 2 m transect per survey. Reports included counts of flowers in the chosen 100-m^2 plots. A photograph of each flower-color category (red, white, pink, purple, blue) was supplied, with a blank spot to fill in the number of anemone flowers counted for this category. Reporters were requested to upload a representative photograph for each of the categories they reported. Finally, the reporters were asked to provide their name, the date of the survey, and its location through the ArcGIS location-based website (Appendix S1: Figure S2). The uploaded photographs were then checked to validate the color categories. The validation revealed that red flowers are visually distinct from all other morphs. Non-red flowers, in contrast, appear in a great variety of intermediate colors, and they cannot always be categorized into discrete color morphs (Figure 1). In addition, some reports were based on a single visit per site and thus did not capture the seasonal changes in the frequencies of color morphs. We therefore pooled all non-red variations of floral colors and refer to them as non-red throughout the study. This citizen science work allowed us to plot the site locations of the color morphs against the mean rainfall. It laid the basis for a detailed monitoring plan, described next.

Flowering phenology of *A. coronaria* along a geographic gradient

We marked two permanent 10 × 10 m plots in each of 18 locations along a ~180-km north–south rainfall gradient (Table 1; map in Figure 1) in November 2021 before the 2021–2022 flowering season. The selected plots represent polymorphic and red flowering sites along the gradient. The plots were placed 5–30 m apart within each site. Each plot was visited every 2 to 3 weeks during the flowering season (December–April of 2021–2022 and 2022–2023). Flowers of each color morph were counted, providing the phenological pattern of each site and red versus non-red composition.

Abiotic conditions along the geographic gradient

Precipitation and temperature data were downloaded from the Israel Meteorological Service (Available at https://ims.gov.il/he/data_gov) climate station nearest to each site. The distance between field sites and the nearest climate stations ranged from 0 to 24 km. Geological properties and soil thickness of the sites were obtained from geological maps of The Geological Survey of Israel (Available at https://egozi.gsi.gov.il/WebApps/Geology/Geo50K_KeyMap/). Five soil samples per site were collected in May 2022. For each sample, organic matter was scraped off the top surface, and 200–500 g of soil from the top 5 cm of soil were collected and stored at room temperature (20°C) in the dark. Subsamples, 200 g from each of five samples, were then pooled, mixed, and analyzed for mineral content (% calcium, nitrogen, phosphorus, potassium, $CaCO_3$), organic matter (%), pH, water saturation (%), electrical conductivity (ds/m), and soil texture (% sand, silt, clay).

Data analyses

Citizen science reports

We tested whether site latitude, longitude, altitude, mean annual temperature, and mean annual rainfall predict population type (red or polymorphic) in the citizen science data set. Altitude was highly correlated with mean temperature (correlation coefficient = −0.70; Appendix S2). We therefore examined the effects of geographic (latitude, longitude, altitude) and climate (temperature, rainfall) variables in two separate models. We used generalized linear models with a binomial distribution of the response variable (red/polymorphic). We weighted the records by the total count of flowers because reports with a higher total of flowers comprise a more representative sample of the population type.

Detailed monitoring of 18 populations

(a) Predicting population type (red or polymorphic): To identify abiotic predictors of red vs. polymorphic populations in this data set, we used additional GLMs with a binomial distribution of the response variable (red/polymorphic). We tested for abiotic explanatory

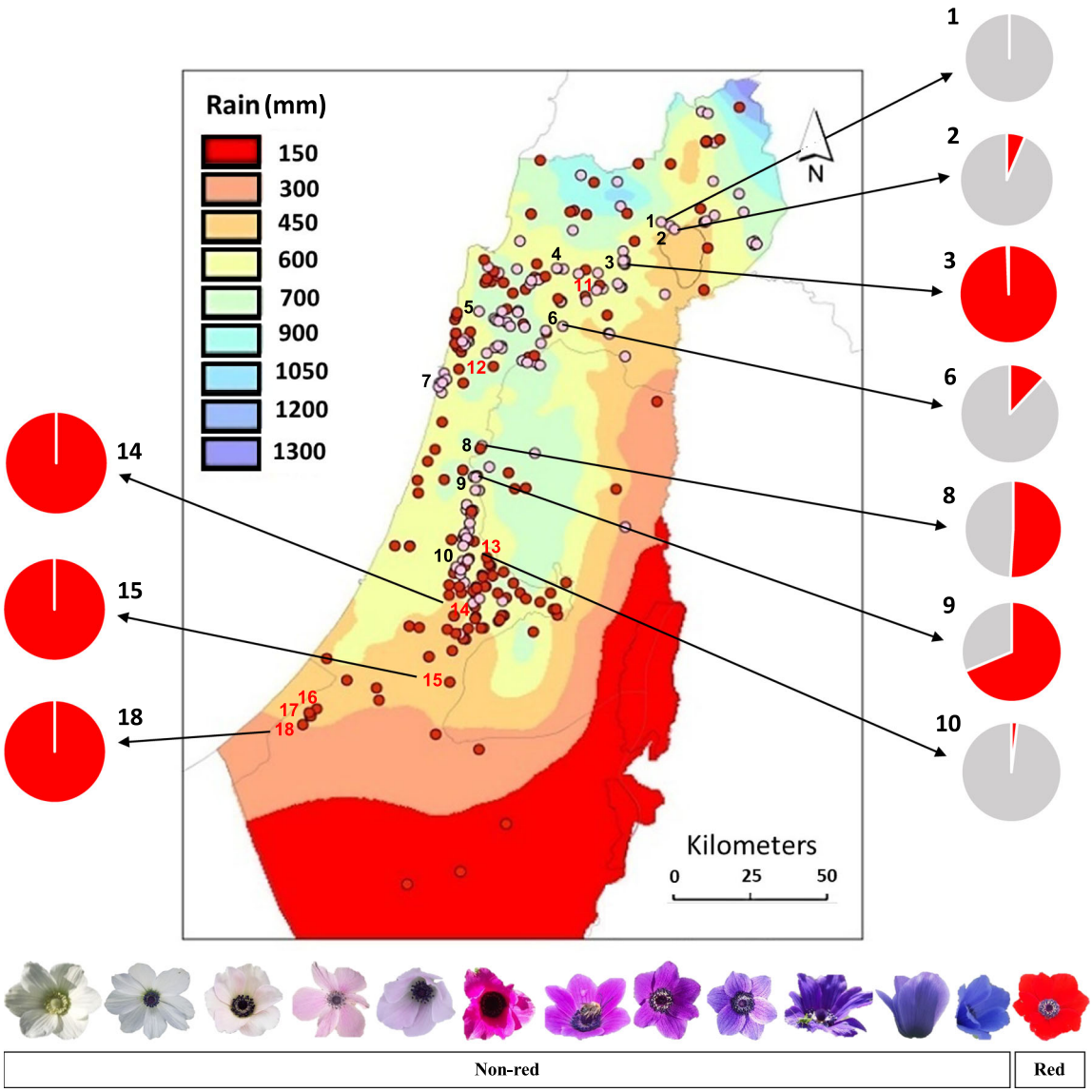

FIGURE 1 Observations of *Anemone coronaria* by citizen scientists in 2019–2020. Red circles denote populations categorized as red. Pink circles denote the presence of non-red flowers, representing polymorphic populations. Background colors indicate average annual rainfall (mm). We monitored 18 populations (Table 1), marked by black (polymorphic) and red (monomorphic) numbers, during the flowering seasons of 2021–2022 and 2022–2023. Flower morph frequencies of seven polymorphic and three red populations at peak bloom, averaged over the two survey years, are plotted as pie charts (red: red flowers, gray: non-red flowers). A catalog of floral colors categorized as red and non-red is provided below the map to illustrate color variations.

variables including multiple soil composition factors and average rainfall. Since the response variable did not vary between years, we excluded explanatory variables that varied annually (such as yearly weather data) from the models.

(b) Predicting flowering phenology: To examine the predictors of flowering phenology, we focused on the timing of flowering onset and the peak of bloom, which varied widely among sites, color morphs, and years. We defined the onset of the flowering season as the first day a flower was observed in our earliest flowering site within a specific flowering season. For each site, we calculated the number of days elapsed between the onset of the flowering season and the first flower in the specific site, which we referred to as "day count" onset of the specific site. First, we examined the phenology within 10 polymorphic sites. We used GLMMs, with site as a random factor, to check for differences in the onset and in the peak flowering time of red versus non-red flowers. Then, using GLM tests, we checked the effects of the following variables on the phenology of the floral morphs across populations and years: average rainfall, accumulated rainfall, soil composition, minimum atmospheric temperature, and average atmospheric temperature. The models created to predict the onset of flowering also tested the effect of the average minimum temperature of the five days preceding the bloom in each site. Models designed to predict the timing of peak flowering also tested the

TABLE 1 Site names, coordinates, altitude, and mean annual rainfall in the 18 monitored populations of *Anemone coronaria*. Numbers correspond to site numbers in Figure 1.

		Coordinates			
Number	**Site**	**N**	**E**	**Altitude (m a.s.l.)**	**Mean rainfall (mm)**
Polymorphic populations					
1	Kahal	32.90299	35.52317	130	508.1
2	Korazim	32.89141	35.55002	−25	589.2
3	Golani	32.77876	35.41338	210	508.6
4	Alonim	32.73044	35.16108	150	606.7
5	Hagit	32.61264	35.03416	120	603.1
6	Megiddo	32.59127	35.23315	50	544.8
7	Olga	32.42305	34.88111	20	474.9
8	Kohav Yair	32.2252	34.99073	70	635.8
9	Rosh Ha'ayin	32.078	34.97349	80	564.4
10	Beko'a	31.82413	34.94359	150	539
Red populations					
11	Sarid	32.66744	35.22973	150	518.9
12	Barkai	32.47085	35.029	75	597.6
13	Beko'a red	31.82488	34.96405	190	539
14	Midras	31.6544	34.94344	290	422.7
15	Pura	31.48885	34.77496	180	366.9
16	Shokeda forest	31.42538	34.50924	120	358.8
17	Be'eri	31.42758	34.46944	100	358.8
18	Lahav	31.3706	34.85915	480	301.6

effect of the average temperature along the flowering season. The factors predicting the onset of bloom were tested separately for red flowers in red and polymorphic populations and for non-red flowers in polymorphic populations. Because the dependent variables (day of flowering onset and flowering peak) varied between years, in this set of models, we entered temperature and rainfall data that were collected separately for each year. Each color-morph–site–year combination comprised a unit of replication for the phenology analyses.

For both sets of models (type of population and timing of flowering), we first tested for correlations between the explanatory variables and excluded multicollinear ones (correlation coefficient >0.55; Appendix S3). We then built full models that included all the retained variables (Appendix S4), and next generated a set of reduced models by excluding one predictor at a time. We chose the best model within each set based on model AIC scores.

We used R packages MASS, ggplot2, ggthemes, dplyr, lmtest, lme4, effectsize, corrplot, reshape2, plotrix, ggplot, patchwork, ggpubr, car, caret, ISLR, and ToothGrowth in R version 4.2.1 (R Core Team, 2022) for the analyses.

RESULTS

Distribution of red and polymorphic populations

Based on 416 observations reported by citizen scientists in 2019–2020, we plotted the geographical distribution of red and polymorphic *A. coronaria* in Israel (Figure 1). Latitude ($F_{1,343} = 27.84$, $P < 0.001$), longitude ($F_{1,343} = 9.64$, $P = 0.002$), and altitude ($F_{1,343} = 4.73$, $P = 0.03$), significantly predicted population type (GLM with binomial distribution; see Appendix S5 for the ANOVA table). Mean annual temperature ($F_{1,344} = 4.60$, $P = 0.03$) and rainfall ($F_{1,344} = 28.85$, $P < 0.001$) were the statistically significant predictors of population type in the climatic model. Notably, color-polymorphic populations and non-red floral morphs were limited to sites with >450 mm annual rainfall (henceforth, the mesic region), whereas red populations and

red floral morphs occurred in both the mesic and the semiarid (annual rainfall <450 mm) regions.

The following sections of the Results are based on detailed monitoring of 18 populations along the climatic gradient during the two flowering seasons.

Soil and climate effects on red and polymorphic populations

The most informative statistical model (based on AIC score) that predicted the population color type (red or polymorphic) included saturation, $CaCO_3$, and silt as explanatory factors (Table 2). The probability of a polymorphic population increased with soil water saturation. On the contrary, higher percentages of $CaCO_3$ and silt in the soil were associated with red populations. Specifically, $CaCO_3$ concentrations above 15% and up to 35% were associated with red populations only (Figure 2).

Flowering phenology

Table 3 shows the following trends: Blooming in the mesic region (>450 mm rain) started 10–13 days earlier than in the semiarid region, and the timing of peak flowering was similar in both regions. In the mesic region, the mean starting day of flowering was similar between years, and the between-year variation in the semiarid populations was larger. The average day of peak flowering varied more between years in the mesic than in the semiarid region.

We also observed some differences between polymorphic and red populations in the timing of flowering, keeping in mind that red populations are present in the whole species range, whereas polymorphic populations are limited to the mesic area. The red populations started to flower 13 days later than polymorphic populations on average. Similarly, red populations reached their peak flowering more than a week later than the polymorphic ones. The red populations varied more between years in blooming onset than did polymorphic populations, but not in the timing of peak bloom (Table 4). Within the 10 polymorphic sites, the mean density of the non-red morphs during their peak flowering time (0.55 flowers/m^2) was approximately half that of the red morph (0.97 flowers/m^2). Non-red flowers in polymorphic populations began blooming significantly earlier than red ($\chi^2_2 = 50.59$, $P < 0.001$) and peaked in the 8th week (Figure 3). The red morph reached its peak significantly later than the non-red, in week 10 ($\chi^2_2 = 15.92$, $P < 0.001$). The non-red floral morphs reached the end of their flowering season almost simultaneously in ~week 12; red ended later in week 14. Accordingly, non-red anemones dominated the color-polymorphic sites early in the season (weeks 1–4), whereas red flowers increased in relative abundance during late season (weeks 11–14) (Figure 3).

TABLE 2 The best generalized linear model (GLM) predicting population color type in the 18 monitored populations of *Anemone coronaria*. Analysis of deviance (type II tests) and effect sizes are reported. *P*-values are based on likelihood ratio tests.

Predictor	χ^2	df	*P*	SD odds ratio	95% CI
Intercept	—	—	—	4.32	[0.26, 762.77]
Saturation	11.22	1	0.0008	196.11	[4.03, 9.72e + 06]
Silt	8.09	1	0.0044	0.0089	[0.00, 0.40]
$CaCO_3$	12.86	1	0.0003	0.01	[0.00, 0.28]

Soil and climate effects on flowering phenology

Next, we explored soil, temperature, and precipitation factors that are potentially associated with the variability in the timing of flowering onset and peak. Soil conductance was significantly and negatively correlated with the day of flowering onset (i.e., the higher the soil conductance, the earlier the onset). It was also the best predictor of the onset day. Other factors had much smaller effects on the timing of onset, as indicated by their lower effect size values (Table 5). For red flowers, the best model also included a significant positive relationship with $CaCO_3$, minimal soil thickness, and rainfall accumulated until the onset day (Table 5). For non-red flowers, the sodium adsorption ratio (SAR), soil texture, and minimal average temperature preceding the onset (Table 5) had additional significant (albeit small) effects on flowering onset.

Peak bloom of red flowers, within polymorphic and red sites, was best explained by the sand concentration in the soil and by the average temperature along the flowering season (Table 5). Sand concentration was higher in red mesic sites and in the semiarid sites consisting of solely red flowers. This high sand concentration was correlated with a later flowering peak in those sites. In the semiarid area, close to the desert, the late flowering peak coincided with warmer temperatures, especially toward the dry season. Overall, as sand concentrations increase, peak flowering occurs later, coinciding with higher average temperatures. The timing of peak flowering in non-red flowers was best explained by potassium and by average temperature. Peak bloom occurred later in sites with higher levels of potassium in the soil and higher average temperatures (Table 5). None of the variables associated with precipitation (mean rainfall, soil saturation, or soil conductance) was a predictor of the timing of peak flowering.

DISCUSSION

Mechanisms that drive and maintain within-population color polymorphism of flowers are intriguing, providing insight into the backbone of the evolutionary process (Sapir et al., 2021). While the major paradigm suggests that

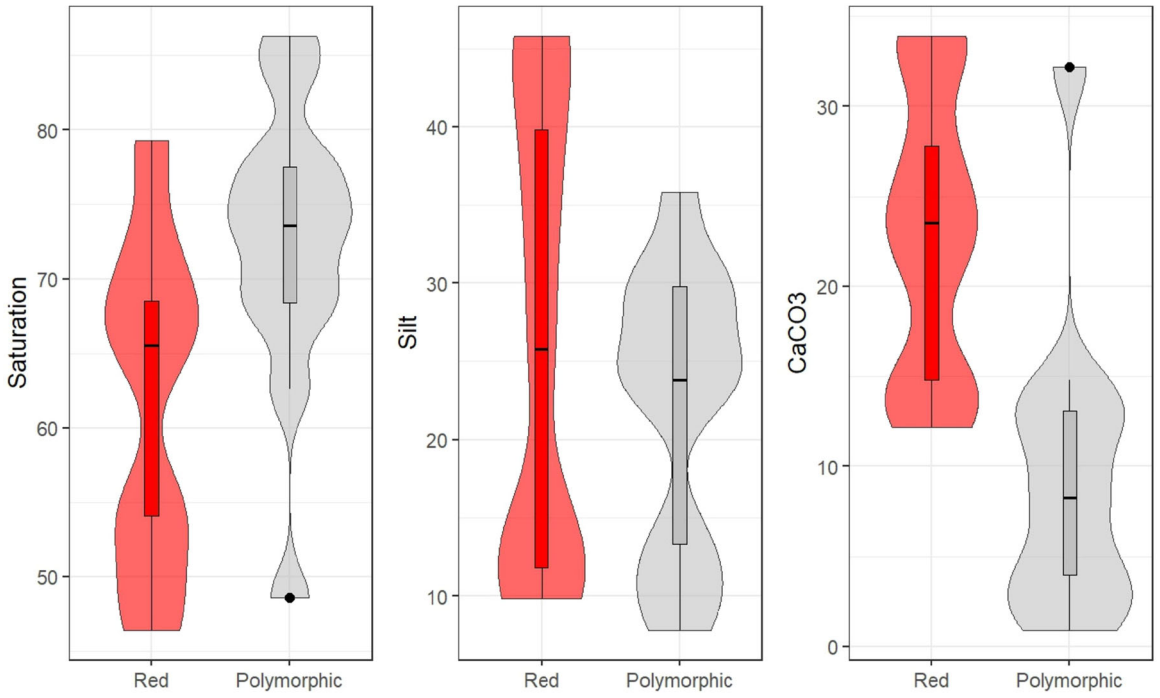

FIGURE 2 Relationships between saturation (left), % silt (center), and $CaCO_3$ soil concentrations (right) and population color type of *Anemone coronaria* in the 18 monitored sites. The violin plot visualizes the data distribution along the *y*-axis. The boxplots within the violins report the central tendency and spread: middle line, median; box edges, 25th and 75th percentiles. The whiskers show the range, excluding extreme outlier values that extend beyond 1.5× the interquartile range from Q1 to Q3. Outlier data appear as dots in the graph.

TABLE 3 Flowering onset and peak days in the monitored populations of *Anemone coronaria* in the mesic and the semiarid regions. The day of flowering onset was calculated for each site in each year as the days elapsed since the first flower was recorded at any site. Peak refers to the day count in which the maximum number of flowers was recorded in each site and year. *N*, number of sites that contributed reliable data regarding onset and peak dates; SE, standard error across sites.

Mesic			Semiarid		
Floral phenology timing	**Year**	**Mean ± SE (*N*)**	**Floral phenology timing**	**Year**	**Mean ± SE (*N*)**
Onset	2022	18.89 ± 4.47 (9)	**Onset**	2022	26.40 ± 7.13 (5)
	2023	19.18 ± 4.34 (11)		2023	33.60 ± 7.78 (4)
Peak	2022	51.85 ± 4.16 (13)	**Peak**	2022	55.71 ± 3.79 (7)
	2023	57.93 ± 3.11 (14)		2023	58.40 ± 5.25 (5)

TABLE 4 Flowering onset and peak days in the monitored mono- and polymorphic populations of *Anemone coronaria*. Onset and peak were calculated as in Table 3.

Polymorphic			Red		
Floral phenology timing	**Year**	**Mean ± SE (*N*)**	**Floral phenology timing**	**Year**	**Mean ± SE (*N*)**
Onset	2022	17.12 ± 4.65 (8)	**Onset**	2022	25.43 ± 5.42 (7)
	2023	15.88 ± 4.51 (9)		2023	33.71 ± 5.52 (7)
Peak	2022	47.08 ± 4.28 (12)	**Peak**	2022	57.50 ± 2.96 (10)
	2023	55.20 ± 3.71 (10)		2023	62.67 ± 3.44 (9)

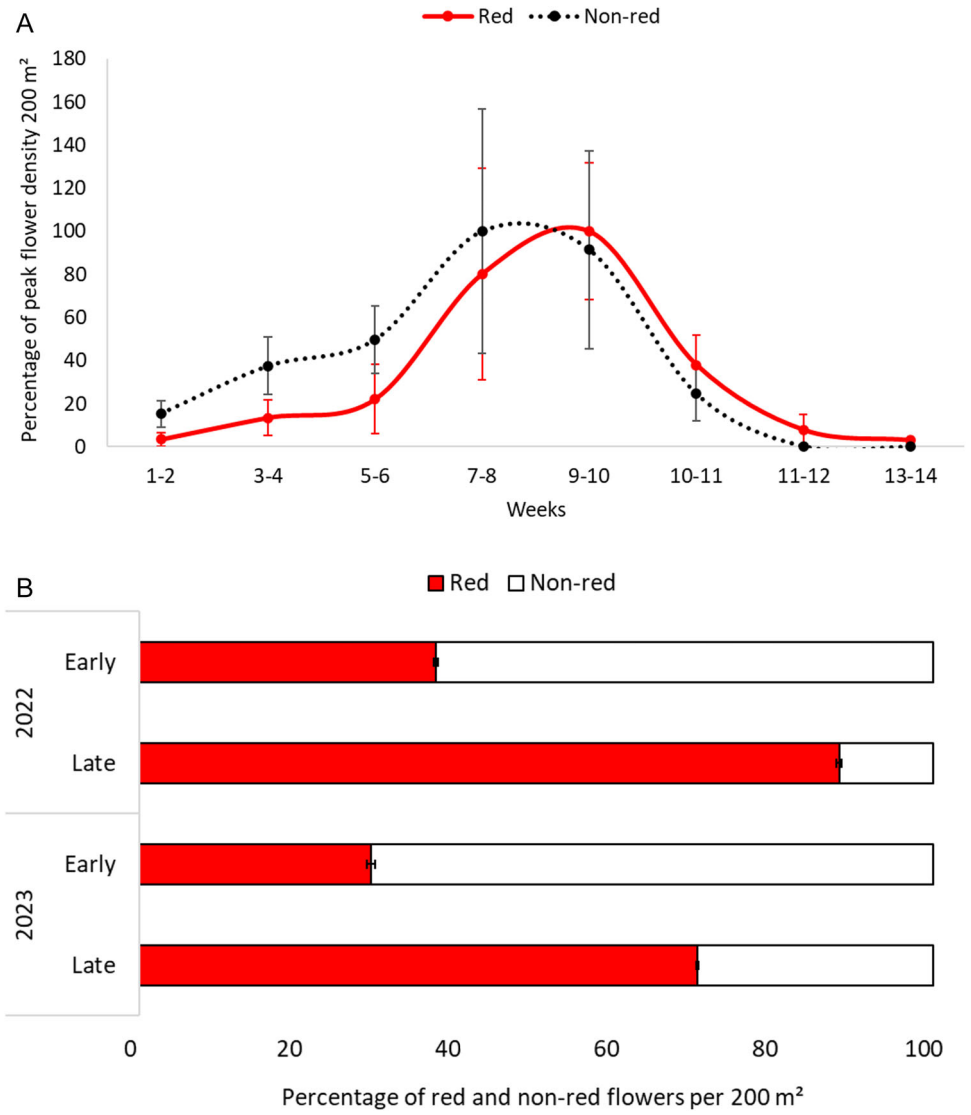

FIGURE 3 (A) *Anemone coronaria* flowering phenology in polymorphic sites based on flower counts in two 100-m^2 squares. The colors represent the floral color morphs (red, red; black, non- red). We averaged color-specific densities in each site, in intervals of 2 weeks and over the 2 years, for all polymorphic sites. We considered the peak average density of flowers from each color morph as 100% and calculated the densities at all other timepoints relative to the peak value. Markers are means, and error bars are standard errors across the 2 years. (B) Percentages of red and non-red *A. coronaria* flowers during the early (weeks 1–4) and late (weeks 11–14) phases of the flowering season. Flower counts of anemones from each color category (red, non-red) were averaged across polymorphic sites for each year. The error bars represent standard errors across the 10 polymorphic sites.

pollinator-mediated balancing selection drives FCP (e.g., Streisfeld et al., 2013; Milano et al., 2016; Lebel et al., 2018; Rodríguez-Castañeda et al., 2024), the association of abiotic factors with spatial variation in FCP deserves attention as well (Schemske and Bierzychudek, 2007). Here we studied *Anemone coronaria*, a species exhibiting spatial and temporal variation in flower color. We combined a citizen-science survey with detailed monitoring of 18 *A. coronaria* populations to identify abiotic predictors of the type of the populations (red vs. polymorphic) and their flowering phenology. In past studies, soil and climate were hypothesized to influence the presence of FCP populations of *A. coronaria* (Horovitz, 1975, 1976; Dafni et al., 2020). Here we examined the correlations between these abiotic factors and FCP quantitatively for the first time.

We also described the flowering phenology of *A. coronaria*'s different morphs and tested these dynamics for correlations with abiotic factors. Differences in flowering phenology between morphs were previously documented in other species with FCP (Arista et al., 2013; Puchałka et al., 2022; Manzanarez-Villasana and Mandujano, 2024; Wang et al., 2024). However, only a handful of studies explored the abiotic variables driving these differences, using either observational (Wang et al., 2024) or experimental (Arista et al., 2013) approaches.

Low water availability was predictive of red populations based on annual mean rainfall data in the citizen science

TABLE 5 The best generalized linear model (GLM) predicting flowering timing (onset/peak) according to flower color-morph. Analysis of deviance table (Type II tests) and effect sizes (standardized odds ratios and standardized incidence rate ratios) are reported. Standardized odds ratios and standardized incidence rate ratios quantify the change in an outcome with a one-unit change in a standardized predictor variable. Ratios that are >1 reflect positive effects, <1 negative effects, and ~1 little to no effects.

Best GLM predicting factors for the flowering onset of red anemones					
Predictor	χ^2	**df**	**Pr(>χ^2)**	**SD odds ratio**	**95% CI**
(Intercept)	—	—	—	26.04	[24.13, 28.05]
Conductance	88.79	1	< 2.200e-16***	0.58	[0.51, 0.65]
$CaCO_3$	22.53	1	2.074e-06***	1.22	[1.12, 1.33]
Soil thickness	24.67	1	6.792e-07***	1.32	[1.18, 1.48]
Accumulated rainfall	1.90	1	0.168	1.05	[0.98, 1.12]
Best GLM predicting factors for the flowering onset of non-red anemones					
Predictor	χ^2	**df**	**Pr(>χ^2)**	**Standardized incidence rate ratio**	**95% CI**
(Intercept)	—	—	—	21.13	[19.48, 22.88]
Conductance	37.58	1	8.783e-10***	0.73	[0.66, 0.81]
$CaCO_3$	3.90	1	0.08	1.11	[1.00, 1.23]
Soil thickness	7.66	1	0.006***	1.13	[1.04, 1.23]
Accumulated rainfall	7.285	1	0.007***	1.11	[1.03, 1.20]
Min temperature	13.199	1	2.801e-4***	0.84	[0.77, 0.92]
Sodium adsorption ratio	5.065	1	0.0244*	1.09	[1.01, 1.18]
Soil texture	9.190	1	0.002***	0.89	[0.82, 0.96]
Best GLM predicting factors for the peak bloom of red anemones and measured effect size					
Predictor	χ^2	**df**	**Pr(>χ^2)**	**Standardized incidence rate ratio**	**95% CI**
(Intercept)	—	—	—	59.12	[56.26, 62.07]
Sand	11.5181	1	0.001***	0.92	[0.87, 0.96]
Temperature (mean)	0.3772	1	0.539	1.02	[0.97, 1.07]
Best GLM predicting factors for the peak bloom of non-red anemones and measured effect size					
Predictor	χ^2	**df**	**Pr(>χ^2)**	**Standardized incidence rate ratio**	**95% CI**
(Intercept)	—	—	—	48.69	[44.81, 52.78]
Potassium	5.4078	1	0.0201*	1.14	[1.02, 1.27]
Temperature (mean)	21.0000	1	4.593e-06***	1.27	[1.15, 1.42]

records and soil saturation in our detailed monitoring of 18 populations. We consider the two data sets as complementary, because the citizen science observations covered a larger number of sites while the population monitoring generated more detailed soil and climate information on fewer sites. In addition, the geographic variables latitude, longitude, and altitude and the climate variable mean temperature predicted the occurrence of red vs. polymorphic populations in the citizen science data set. Statistical modeling of the population-monitoring data set suggests high $CaCO_3$ and silt contents in the soil as predictors of red populations. These soil variables may also be associated with low water availability to plants (Appendix S3) because they contribute to soil crusts that reduce water infiltration (Wahba et al., 2019; Lin et al., 2025). Polymorphic populations were limited to soils with water saturation above 60%, rainfall above 450 mm annual, and $CaCO_3$ below 15%, except for site 10 (Beko'a polymorphic). This site is situated at the southern edge of the polymorphic populations and showed outlier results.

Red flowers started flowering later than non-red flowers (Figure 3). In semiarid areas, where the populations are exclusively red, flowering started later than in the mesic locations (Table 3). These trends suggest environmental control over the onset of flowering, which possibly differs between color morphs. High electrical conductivity of the

soil was the main predictor of an earlier onset of flowering in all color morphs. Interpreting this effect is not straightforward, because conductivity combines soil salinity, texture, and water content. Nevertheless, it hints at a possible role of water availability (possibly combined with ion concentrations) in regulating the onset of flowering. Rainfall was indeed previously reported to regulate flowering phenology in some Mediterranean ecosystems (Peñuelas et al., 2004; Donoso et al., 2016). In addition, the flowering onset of red flowers was delayed with increasing $CaCO_3$ soil concentrations, suggesting an additional explanation for the late flowering of the red populations in the semiarid areas, because soils in arid and semiarid environments often contain >15% $CaCO_3$. Such high calcium carbonate levels are linked to low water availability for plants, low organic matter, and reduced micronutrients such as potassium (Wahba et al., 2019; Appendix S3). For the non-red flowers, the sodium adsorption ratio (SAR), the sodium amount (Na) relative to calcium (Ca) and magnesium (Mg) in water extracted from saturated soil paste, was also an important predictor. Overall, these findings reflect the importance of water and nutrient availability in the soil. Their interaction contributes to soil conductance, which was predictive of the flowering onset of non-red flowers.

Mean site temperature was a predictor of the timing of peak flowering in both red and non-red flowers, in line with abundant previous evidence for the role of temperature as a flowering signal (Keasar and Labin, 2025). Additionally, high sand concentration in the soil was predictive of earlier peak flowering in red flowers, linked to their shorter blooming duration. Early flowering peak in sandy soils might be related to the high thermal conductivity (the ability to conduct/transfer heat) generated by sand due to its quartz component. The peak flowering of non-red plants occurred later in sites with higher soil potassium levels and higher average temperatures. Mean temperature had a stronger effect. Interestingly, no variable related to water availability (rainfall, soil saturation, soil conductance) was a significant predictor of peak flowering, suggesting that the abiotic cue for peak flowering is different from the cue for flowering onset.

Our previous work showed that the pollinators of *A. coronaria*, some of which also act as herbivores, vary among color morphs and geographically and temporally (Saabna et al., 2025; T. Labin et al., unpublished data). Here, we found that abiotic factors, which vary over space and time, were also predictors of population phenology and whether they are color polymorphic. Previous studies describe links between environmental stressors and high floral pigment concentrations (Dick et al., 2011; Ortiz et al., 2015; Berardi et al., 2016), as opposed to lower tolerance of white and unpigmented flowers (Coberly and Rausher, 2003; Tang and Huang, 2010; Tang et al., 2016). These links suggest climatic and edaphic adaptations as possible drivers of geographic segregation of color morphs (Schemske and Bierzychudek, 2007; Dick et al., 2011; Arista et al., 2013). We propose that biotic and abiotic variables shape the spatio-temporal pattern of FCP in *A. coronaria* by interacting with the flowering phenology: Red populations are better adapted to xeric conditions, which occur in semiarid sites and toward the end of the flowering season. They tend to have a shorter flowering duration, and their late bloom coincides with the activity period of glaphyrid beetles, their main pollinator. The red flowers gain most of their pollinator visits during peak and late season in the semiarid area (Keasar et al., 2010; T. Labin et al., unpublished data). Non-red flowers, on the other hand, perform better under more mesic conditions. These morphs also attract bees and flies, which are the main pollinators of *A. coronaria* in wetter sites and early in the flowering season, when rain is more abundant (Dafni et al., 2020; T. Labin et al., unpublished data;). Altogether, we propose that the abiotic predictors of flowering phenology interact with pollinator availability to promote early-season flowering of non-red anemones in mesic sites, and late-season flowering of red flowers in semiarid sites. All floral color morphs overlap in their bloom in mid season, generating opportunities for gene exchange between color morphs during this period of time. We thus propose that biotic and abiotic selection pressures drive the geographic distribution of polymorphic vs. monomorphic populations and their different flowering phenology. Although we were unable to estimate the relative contribution of biotic vs. abiotic factors using our current data set, theoretical modeling predicts that pollinators are stronger selective agents for FCP than agents that affect plant survival in their vegetative phase (Tenhumberg et al., 2023). We are currently testing this prediction through a common-garden experiment that manipulates the water supply to plants of *A. coronaria* while keeping the pollinator community the same.

Narbona et al. (2017) pointed out that all cases of FCP in the Mediterranean combine both mono- and polymorphic populations. They referred to the Mediterranean basin as an area of geographic mosaics, tying polymorphism to the high heterogeneity of climate, orography, soils and pollinator composition in Mediterranean ecosystems. Under such heterogeneous conditions, theoretical models predict higher stability, persistence and larger range expansion and evolutionary potential to polymorphic species when color morphs are associated with traits affecting fitness (Forsman et al., 2008). Our case exemplifies the complexities faced by a widespread species in the Mediterranean basin considering the variation in abiotic conditions between years and areas.

From a wider perspective, our findings raise thoughts about plant traits that may confer adaptations to global warming. Specifically in *A. coronaria*, future research could further investigate whether the red morph is more resilient to climate change than the non-red morph and how the distribution of the morphs and their pollinator assemblages may change as the climate warms. Modelling different climate scenarios and considering the temperature requirements of the color morphs could allow the prediction of the future distribution of the flower color polymorphism of *A. coronaria*. Predictions of future distribution and information about the differences in the phenology between color morphs could be used to project their

possible eventual reproductive isolation. These are just some of the topics yet to be explored.

CONCLUSIONS

The geographic pattern of flower color polymorphism in *Anemone coronaria* is governed by abiotic factors, mostly water availability, soil saturation, its $CaCO_3$ content, and silt. The flowering phenology of the different color morphs was found to be governed mostly by mean temperature, soil conductivity, sodium adsorption ratio, and the concentrations of sand, $CaCO_3$, and potassium in the soil. The flowering phenology in turn interacts with the pollinator community (T. Labin et al., unpublished manuscript). This evidence supports the broadening of the pollinator-mediated paradigm, which is often proposed as the major driver of flower color polymorphism. As mechanisms that drive and maintain flower color polymorphism vary among plant species, abiotic factors should be incorporated into studies that are aimed at understanding the evolution of flower color polymorphism.

AUTHOR CONTRIBUTIONS

Y.S., T.K., and N.L.A. established the citizens science project and curated the data. Y.S. and T.K. obtained funding. Y.S. and T.K. conceived and established the detailed phenology project. T.L., Y.S., T.K., and B.P. collected field data. T.L., T.K., and Y.S. analyzed the data. T.L. and T.K. led the writing of the manuscript, Y.S. commented on and edited early drafts, and all authors reviewed and approved the final version.

ACKNOWLEDGMENTS

We thank many colleagues and friends: Yosef Labin, Rafi Friedman, Tzafrir Tiferet, Neta Damary, and Norah Saabna were committed field assistants; Yamit Bar-Lev provided administrative help; Ofri Eitan helped collect and manage data; Or-Leyl Har-Edom assisted with GIS analyses; Avi Shmida supplied detailed spatial information on polymorphic anemone populations; Johannes Spaethe, Casper van der Kooi, Jonathan Heinze, and the Keasar and Sapir lab members contributed to discussions of the results. The Israel Nature and Parks Authority and the Department of forestry (KKL-JNF) provided permits (Permit 2022/42940) and help in field sites, and the Society for Protection of Nature in Israel supplied the citizens science platform. We extend a special thank you to each citizen who took time to report on anemones and contribute to this study. We thank the reviewers and editors of this special issue of *American Journal of Botany* for their suggestions and contributions, which significantly improved the text. The work was supported by a DFG - Deutsche Forschungsgemeinschaft grant (no. GZ: SP 1380/2-1) to Johannes Spaethe, Y.S., and T.K., and by a Ph.D. scholarship to T.L. from the University of Haifa.

DATA AVAILABILITY STATEMENT

All data used for the paper is deposited in Zenodo: https://doi.org/10.5281/zenodo.15767948.

ORCID

Tzlil Labin https://orcid.org/0009-0007-7113-1226
Banisha Phukela https://orcid.org/0000-0003-3028-6348
Tamar Keasar https://orcid.org/0000-0002-4925-0823
Nirit Lavie-Alon https://orcid.org/0000-0002-6136-4209
Yuval Sapir https://orcid.org/0000-0001-9685-8076

REFERENCES

Arista, M., M. Talavera, R. Berjano, and P. L. Ortiz. 2013. Abiotic factors may explain the geographical distribution of flower colour morphs and the maintenance of colour polymorphism in the scarlet pimpernel. *Journal of Ecology* 101: 1613–1622.

Berardi, A. E., P. D. Fields, J. L. Abbate, and D. R. Taylor. 2016. Elevational divergence and clinal variation in floral color and leaf chemistry in *Silene vulgaris*. *American Journal of Botany* 103: 1508–1523.

Bolton, P. E., L. A. Rollins, and S. C. Griffith. 2015. The danger within: the role of genetic, behavioural and ecological factors in population persistence of colour polymorphic species. *Molecular Ecology* 24: 2907–2915.

Coberly, L. C., and M. D. Rausher. 2003. Analysis of a chalcone synthase mutant in *Ipomoea purpurea* reveals a novel function for flavonoids: amelioration of heat stress. *Molecular Ecology* 12: 1113–1124.

Dafni, A., H. Tzohari, R. Ben-shlomo, N. J. Vereecken, and G. Ne'eman. 2020. Breeding system and gene flow in *Anemone coronaria*. *Plants* 9: 397.

Dai, W., Y. Yang, H. M. Patch, C. M. Grozinger, and J. Mu. 2022. Soil moisture affects plant–pollinator interactions in an annual flowering plant. *Philosophical Transactions of the Royal Society, B: Biological Sciences* 377: 20210423.

Dick, C. A., J. Buenrostro, T. Butler, M. L. Carlson, D. J. Kliebenstein, and J. B. Whittall. 2011. Arctic mustard flower color polymorphism controlled by petal-specific downregulation at the threshold of the anthocyanin biosynthetic pathway. *PLoS One* 6: e18230.

Donoso, I., C. Stefanescu, A. Martínez-Abraín, and A. Traveset. 2016. Phenological asynchrony in plant–butterfly interactions associated with climate: a community-wide perspective. *Oikos* 125: 1434–1444.

Gonzalez, A. 2009. Pigment loss in response to the environment: A new role for the WD/bHLH/MYB anthocyanin regulatory complex. *New Phytologist* 182: 1–3.

Forsman, A., J. Ahnesjö, S. Caesar, and M. Karlsson. 2008. A model of ecological and evolutionary consequences of color polymorphism. *Ecology* 89: 34-40.

Horovitz, A. 1976. Edaphic factors and flower colour distribution in the Anemoneae (Ranunculaceae). *Plant Systematics and Evolution* 126: 239–242.

Horovitz, A. 1985. *Anemone coronari*a and related species. *In* A. H. Halevy [ed.], Handbook of flowering, 455–464. CRC Press, Boca Raton, FL, USA.

Horovitz, A. 1991. The pollination syndrome of *Anemone coronaria* L.; an insect-biased mutualism. *Acta Horticulturae* 288: 283-287.

Horovitz, A. 1995. The local gene pool of *Anemone coronaria*. *Acta Horticulturae* 420: 144–146.

Horovitz, A., J. Galil, and D. Zohary. 1975. Biological flora of Israel. VI. *Anemone coronaria* L. *Israel Journal of Botany* 24: 26–41.

Imbert, E. 2021. Spatial distribution of flower colour polymorphism in *Iris lutescens*. *Botany Letters* 168: 408-421.

Keasar, T., A. Harari, R. Sabatinelli, G. Keith, D. Dafni, A. Shavit, O. A. Zylberthal, and A. Shmida. 2010. Red anemone guild flowers as focal places for mating and feeding by Levant glaphyrid beetles. *Biological Journal of the Linnean Society* 99: 808-817.

Keasar, T., and T. Labin. 2025. Are you in synch? How the timing of plant and insect life-history events affects pollination interactions. *In* M. Segoli and E. Wajnberg [eds], Life history evolution: traits, interactions, and applications, 285–296. Wiley, Hoboken, NJ, USA.

Koes, R. E., F. Quattrocchio, and N. M. Mol Joseph. 1994. The flavonoid biosynthetic pathway in plants: function and evolution. *BioEssays* 16: 123–132.

Lebel, M., U. Obolski, L. Hadany, and Y. Sapir. 2018. Pollinator-mediated selection on floral size and tube color in *Linum pubescens*:

Can differential behavior and preference in different times of the day maintain dimorphism? *Ecology and Evolution* 8: 1096-1106.

Lin, L., P. Y. Lonla, J. Vijayakumar, M. K. Khan, G. Di Emidio, N. Krekelbergh, A. Verdoodt., and W. Cornelis. 2025. Soil surface properties and infiltration response to crust forming of a sandy loam and silt loam. *Soil and Tillage Research* 248: 106440.

Manzanarez-Villasana, G., and M. C. Mandujano. 2024. Morphological and phenological variation of flower colour morphs in a wild population of *Opuntia streptacantha* (Cactaceae). *Plant Ecology and Evolution* 157: 244-255.

Milano, E. R., A. M. Kenney, and T. E. Juenger. 2016. Adaptive differentiation in floral traits in the presence of high gene flow in scarlet gilia (*Ipomopsis aggregata*). *Molecular Ecology* 25: 5862-5875.

Mtileni, M. P., N. C. Le Maitre, S. Steenhuisenand K. L. Glennon. 2024. Increased solar radiation and soil moisture determine flower colour frequency in a mountain endemic plant population. *Plant Ecology* 225: 201-211.

Narbona, E., H. Wang, P. L. Ortiz, M. Arista, and E. Imbert. 2017. Flower colour polymorphism in the Mediterranean Basin: occurrence, maintenance and implications for speciation. *Plant Biology* 20: 8-20.

Ortiz, P. L., R. Berjano, M. Talavera, and M. Arista. 2015. Flower colour polymorphism in *Lysimachia arvensis*: How is the red morph maintained in Mediterranean environments. *Perspectives in Plant Ecology, Evolution and Systematics* 17: 142–150.

Peach, K., J. W. Liu, and S. J. Mazer. 2020. Climate predicts UV floral pattern size, anthocyanin concentration, and pollen performance in *Clarkia unguiculata*. *Frontiers in Plant Science* 11: 847.

Peñuelas, J., I. Filella, X. Zhang, L. Llorens, R. Ogaya, F. Lloret, P. Comas, et al. 2004. Complex spatiotemporal phenological shifts as a response to rainfall changes. *New Phytologist* 161: 837–846.

Puchałka, R., M. Klisz, S. Koniakin, P. Czortek, Ł. Dylewski, S. Paź-Dyderska, M. Vítková, et al. 2022. Citizen science helps predictions of climate change impact on flowering phenology: A study on Anemone nemorosa. *Agricultural and Forest Meteorology* 325: 109133.

R Core Team. 2022. R: A language and environment for statistical computing. R Foundation for Statistical Computing, Vienna, Austria. https://www.R-project.org/.

Rodríguez-Castañeda, N. L., M. L. Buide, M. Arista, E. Narbona, and P. L. Ortiz. 2024. Pollinator response to yellow UV-patterned versus white UV-patternless flower dimorphism in *Anemone palmata*. *Plant Biology* 26: 929–943.

Rudall, P. J. 2019. Colourful cones: How did flower colour first evolve? *Journal of Experimental Botany* 71: 759–767.

Saabna, N., T. Keasar, and Y. Sapir. 2025. The roles of florivory and herbivory in maintaining intra-population flower colour variation in *Anemone coronaria*. *Plant Biology* 27: 163–171.

Sapir, Y., M. K. Gallagher, and E. Senden. 2021. What maintains flower colour variation within populations? *Trends in Ecology and Evolution* 36: 507–519.

Schemske, D. W., and P. Bierzychudek. 2007. Spatial differentiation for flower color in the desert annual *Lianthus parryae*: Was Wright right? *Evolution* 61: 2528–2543.

Strauss, S. Y., and J. B. Whittall. 2016. Non-pollinator agents of selection on floral traits: Ecology and evolution of flowers. *In* L. D. Harder and S. C. H. Barrett [eds.], 120–138. Oxford University Press, Oxford, UK.

Streisfeld, M. A., W. N. Young, and J. M. Sobel. 2013. Divergent selection drives genetic differentiation in an R2R3-MYB transcription factor that contributes to incipient speciation in *Mimulus aurantiacus*. *PLoS Genetics* 9: e1003385.

Sullivan, C. N. and M. H. Koski. 2021.The effects of climate change on floral anthocyanin polymorphisms. *Proceedings of the Royal Society, B: Biological Sciences* 288: 20202693.

Tang, X., and S. Huang. 2010. Fluctuating selection by water level on gynoecium colour polymorphism in an aquatic plant. *Annals of Botany* 106: 843–848.

Tang, X., H. Liu, C. Zhang, Y. Wang, X. Zhang, and Y. Yi. 2016. Flower colour polymorphism in *Geranium nepalense* (Geraniaceae): adaptation to non-pollinator agents. *Polish Journal of Ecology* 64: 526–533.

Tenhumberg, B., A. S. Dellinger, and S. D. Smith. 2023. Modelling pollinator and nonpollinator selection on flower colour variation. *Journal of Ecology* 111: 746-760.

Trunschke, J., K. Lunau, G. H. Pyke, Z. X. Ren, and H. Wang. 2021. Flower color evolution and the evidence of pollinator-mediated selection. *Frontiers in Plant Science* 12: 617851.

Vaidya, P., A. McDurmon, E. Mattoon, M. Keefe, L. Carley, C.R. Lee, R. Bingham, and J. T. Anderson. 2018. Ecological causes and consequences of flower color polymorphism in a self-pollinating plant (*Boechera stricta*). *New Phytologist* 218: 380–392.

Wahba, M., L. A. B. İ. B. Fawkia, and A. Zaghloul. 2019. Management of calcareous soils in arid region. *International Journal of Environmental Pollution and Environmental Modelling* 2: 248-258.

Wang, X., H. Tang, and Y. Liu. 2024. Maintenance of flower color dimorphism in *Ophiorrhiza japonica* (Rubiaceae): responses to fluctuating temperatures in a dolomite Karst region. *Frontiers in Plant Science* 15: 1495112.

Winkel-Shirley, B. 2002. Biosynthesis of flavonoids and effects of stress. *Current Opinion in Plant Biology* 5: 218-223.

Yonash N., J. Fang, A. Shamay, N. Pollak, U. Lavi, A. Cohen. 2004. Phenotypic and genotypic analysis of a commercial cultivar and wild populations of *Anemone coronaria*. *Euphytica* 136: 51–62.

SUPPORTING INFORMATION

Additional supporting information can be found online in the Supporting Information section at the end of this article.

Figure S1. Translated version of the Hebrew citizens science reporting website. Available at: https://www.teva.org.il/citizen-science/3389

Figure S2. Translated version of the Hebrew citizens science report form. Available at: https://survey123.arcgis.com/share/576930682b814eebb531fcd4b7b1101f.

Appendix S1. Screen shots of the citizens science website site and reporting form, translated to English.

Appendix S2. Correlations between the geographic and climate variables based on citizen science data.

Appendix S3. Correlations between abiotic variables (soil properties and average rainfall) assessed for the 18 monitored populations.

Appendix S4. Explanatory variables tested in the full GLM models for the 18 monitored populations.

Appendix S5. Predictors of population type (red/polymorphic) based on the citizens' science data set.

How to cite this article: Labin, T., B. Phukela, T. Keasar, N. Lavie-Alon, and Y. Sapir. 2026. Color polymorphism in *Anemone coronaria*: Correlations with soil, climate, and flowering phenology. *American Journal of Botany* 113(1): e70093. https://doi.org/10.1002/ajb2.70093